Formation of Polymeric Foams from Aqueous Foams Stabilized Using a Polymerizable Surfactant

W. R. PALANI RAJ, MOHAN SASTHAV, and H. MICHAEL CHEUNG*

Department of Chemical Engineering, The University of Akron, Akron, Ohio 44325-3906

SYNOPSIS

Polymerization of foams formed by purging with nitrogen an aqueous precursor system made up of a polymerizable surfactant, a monomer, and a cross-linking agent yielded stable polymeric foams. The precursor system for foaming contained hydrophobic components (methyl methacrylate as monomer and ethylene glycol dimethacrylate as cross-linking agent) in water and was stabilized using the polymerizable surfactant potassium acrylamidostearate. The phase-behavior study for the precursor system was conducted followed by an investigation of the stability of the foams obtained on purging with nitrogen. Sonicating the precursor systems during the process of purging with nitrogen gas followed by polymerization resulted in aqueous foams having a uniform cell size. The aqueous foams were polymerized by a free-radical mechanism using photoinitiated and thermal techniques to form stable polymeric foams. The morphology and density of the polymeric foams obtained was determined and observed to be significantly dependent on the composition of the aqueous precursor that was foamed. These results indicate the feasibility of synthesizing polymeric foams without using hydrocarbon solvents or blowing agents during polymerization. © 1993 John Wiley & Sons, Inc.

INTRODUCTION

The technique most widely used to prepare macrocellular polymer foams (cell sizes of 100 μm or more) is the expansion process in which a gaseous phase causes pore formation and growth of pores in the polymer matrix followed by stabilization of the cellular structure by physical or chemical means.[1] Some of the other techniques that are used include sintering of small particles[1] and leaching of soluble materials dispersed in a polymer matrix.[2] Some of the methods used for making microcellular polymeric foams (cell sizes 10 μm or lower) have been controlled phase separation from polymer solutions,[3-5] reaction-induced phase separation starting from monomer solutions,[6-8] and polymerization of high internal phase emulsions (HIPE)[9-15] or microemulsions.[23-26] The last two processes mentioned are of relatively recent origin and utilize surfactants to form microstructured monomer containing systems that are then polymerized to form microporous polymeric materials. The HIPE and microemulsion routes represent an attempt to "lock in" the microstructure of the precursor by polymerization, followed by removal of the unpolymerized aqueous phase to yield a microporous polymer.

The formation of foams from surfactant-based systems as precursors is an area of active research interest.[9-15,23-26] These published studies have indicated the feasibility of obtaining microporous polymeric foams by polymerizing monomer systems that have been stabilized using surfactants. The present work represents an extension of our research in the area of polymerizing surfactant-based microstructured media.[23-26] In contrast to earlier studies with surfactant-based precursors that were directed toward formation of microporous polymeric materials,[9-15,23-26] the present study relates to synthesizing macroporous foams from precursors stabilized using surfactants.

In the earlier studies, the surfactant used to form the microstructured precursor was generally not polymerizable and it existed as an unpolymerized component in the polymeric foam obtained. In this

* To whom correspondence should be addressed.

Journal of Applied Polymer Science, Vol. 49, 1453-1470 (1993)
 CCC 0021-8995/93/081453-18

study, a polymerizable surfactant (potassium acrylamidostearate) was used to form macroporous poly(methyl methacrylate) foams. The rationale in using a polymerizable surfactant was to avoid the presence of unpolymerized surfactant in the polymeric foam. This was achieved by copolymerization of the polymerizable surfactant.

A novel route to obtaining a macroporous polymeric foam by polymerizing an aqueous foam formed by bubbling a gas through an aqueous precursor containing the polymerizable components was examined in this study. The aqueous foams were formed by purging, with nitrogen, aqueous systems containing the monomer, cross-linking agent, and surfactant. The aqueous systems were also sonicated during the process of purging with nitrogen. The aqueous foams from certain compositions were sufficiently stable and could be polymerized to yield rigid open-cell polymeric foams. Free-radical polymerization of the aqueous foam using AIBN as the initiator was activated with ultraviolet radiation and completed by a thermal technique. The morphology of the polymeric foams was investigated by scanning electron microscopy and was found to be strongly dependent on the composition of the precursor system. The cell size, the openings in the cells, and the density of the polymeric foam could be controlled by variations in the composition of the precursor.

EXPERIMENTAL

Materials

Methyl methacrylate (MMA), ethylene glycol dimethacrylate (EGDMA), acrylonitrile, acetone, carbon tetrachloride, and potassium hydroxide were obtained from Aldrich and were of purity greater than 99%. The water was used deionized and doubly distilled. Oleic acid was of 99% purity and was obtained from Fisher.

Synthesis of Polymerizable Surfactant

The polymerizable surfactant potassium acrylamidostearate (KAAS) was synthesized using the modified Ritter reaction.[16,17,20] Acylamidostearic acid (AAS) was first synthesized. In a three-necked flask fitted with a stirrer and a dropping funnel using a constant temperature bath, 242 g of 98% sulfuric acid was cooled to 5°C. Acrylonitrile, 106 g, was added and the temperature maintained at 5°C. Oleic acid, 141 g, was added dropwise, taking care to maintain the temperature below 10°C. The sample was agitated for 12 h at 10°C and the temperature was allowed to rise to 25°C at the end of the period. A brown viscous liquid was obtained that was added to a trough containing 1.5 L of water and ice, maintaining the temperature below 10°C. The temperature was allowed to rise to 25°C slowly with the melting of ice and the mixture was agitated for 10 h. The water was replaced every hour during this period to wash off the sulfuric acid. The product, AAS, was obtained as a pale yellow paste. AAS was washed with carbon tetrachloride followed by cyclohexane and then with acetone and dried at 25°C. To prepare KAAS, AAS was neutralized with an aqueous solution of potassium hydroxide. The aqueous solution of KAAS was dried to obtain the surfactant as a powder.

IR Spectroscopy

The IR spectra of the surfactant KAAS and its homopolymer were obtained by forming KBr pellets. The surfactant or polymer was mixed with potassium bromide to the extent of less than 0.1% by weight and pelletized using a hydraulic press. The KBr pellet obtained was examined using a Bio-Rad Model FTS-7 FTIR and the IR spectra of the surfactant or polymer was recorded.

Phase-behavior Studies

Samples for phase-behavior studies were prepared by adding the required amounts of the various components into clean glass tubes, which were then sealed. The compositions used throughout the study were on a weight percent basis. EGDMA added was always 5% by weight of MMA. The samples were hand-shaken, followed by sonication for 10 min. The samples were then equilibrated in a constant temperature water bath for 48 h at 25 ± 0.1°C before making measurements. The criterion for equilibrium was the reproducibility of phases in shaking and standing cycles.

Surface Tension Measurement

Surface tension was measured with a Kruss Interfacial-Tensiometer K8 with a provision to control the sample temperature. Measurement of the critical micelle concentration (CMC) of the surfactant was carried out using aqueous solutions of known concentration. The measurements were checked several times to ensure reproducibility.

Viscosity Measurements

The viscosity measurements were made using a Brookfield LVT digital viscometer having a small

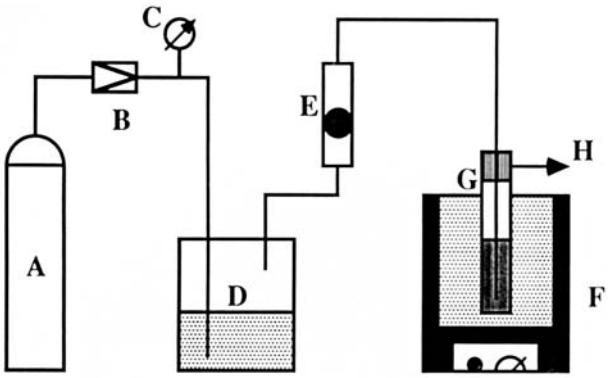

Figure 1 Experimental setup for forming aqueous foams: (A) nitrogen gas tank; (B) pressure regulator; (C) pressure gauge; (D) humidifier; (E) flowmeter; (F) sonicator; (G) sample tube; (H) gas vent.

sample adaptor with a provision to control the sample temperature. The measurements were made at 25°C at a shear rate of 12/s.

Experimental Arrangement for Foaming

The experimental setup for foaming is shown in Figure 1. Nitrogen gas at a flow rate of 5 mL/min was purged through the sample contained in a 16 mm-diameter tube using a 18 gauge stainless-steel capillary. The sample tube was placed in a Cole-Parmer Model 8851 sonicator bath and the sample was sonicated continuously at 47 kHz with 115 W while being purged using nitrogen. The sample was purged for a duration of 10 min.

The stability of the foam generated was determined from the measurement of the reduction in foam height with time. The criterion for classifying a foam as stable was a reduction in foam height of less than 25% during the first hour.

Polymerization Procedure

Polymerization of the aqueous foams was carried out using AIBN as the initiator. The polymerization initiator was added to the precursor prior to foaming with nitrogen. The amount of initiator used was 0.2% by weight. Photoinitiated polymerization of the aqueous foam was carried out in a reaction cell[24] using a 450 W ultraviolet source for a duration of 1 h. The temperature in the reaction cell was maintained at 25 ± 0.1°C during the course of polymerization by means of circulation of coolant water in the reaction cell. The sample tube was then transferred to an oven maintained at a temperature of 55°C and the polymerization was completed over a 24 h period. AIBN can be activated by ultraviolet

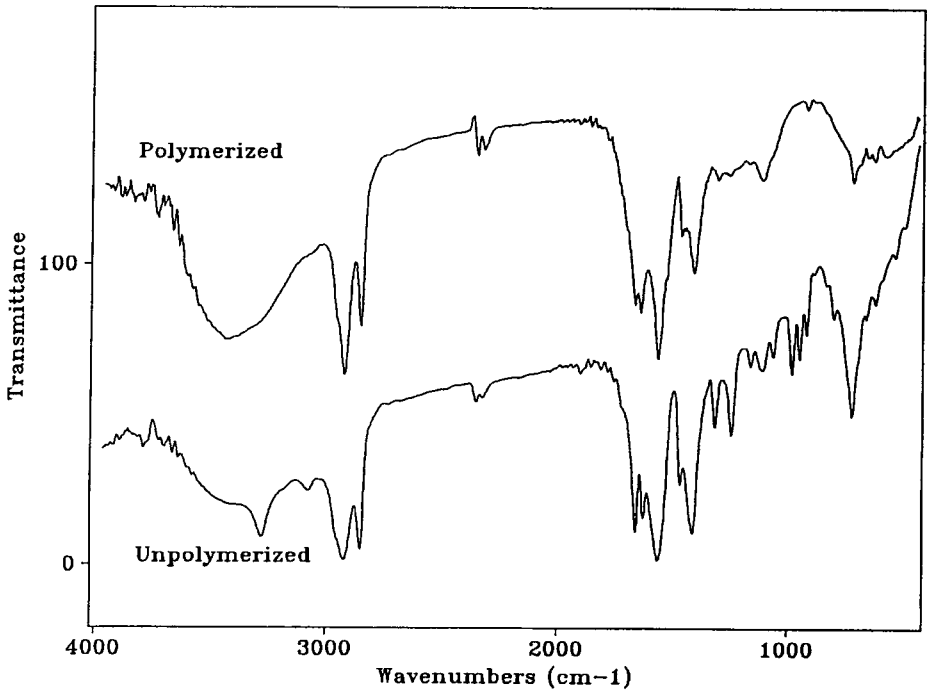

Figure 2 FTIR spectra of the surfactant KAAS before polymerization and the homopolymer formed from KAAS after polymerization.

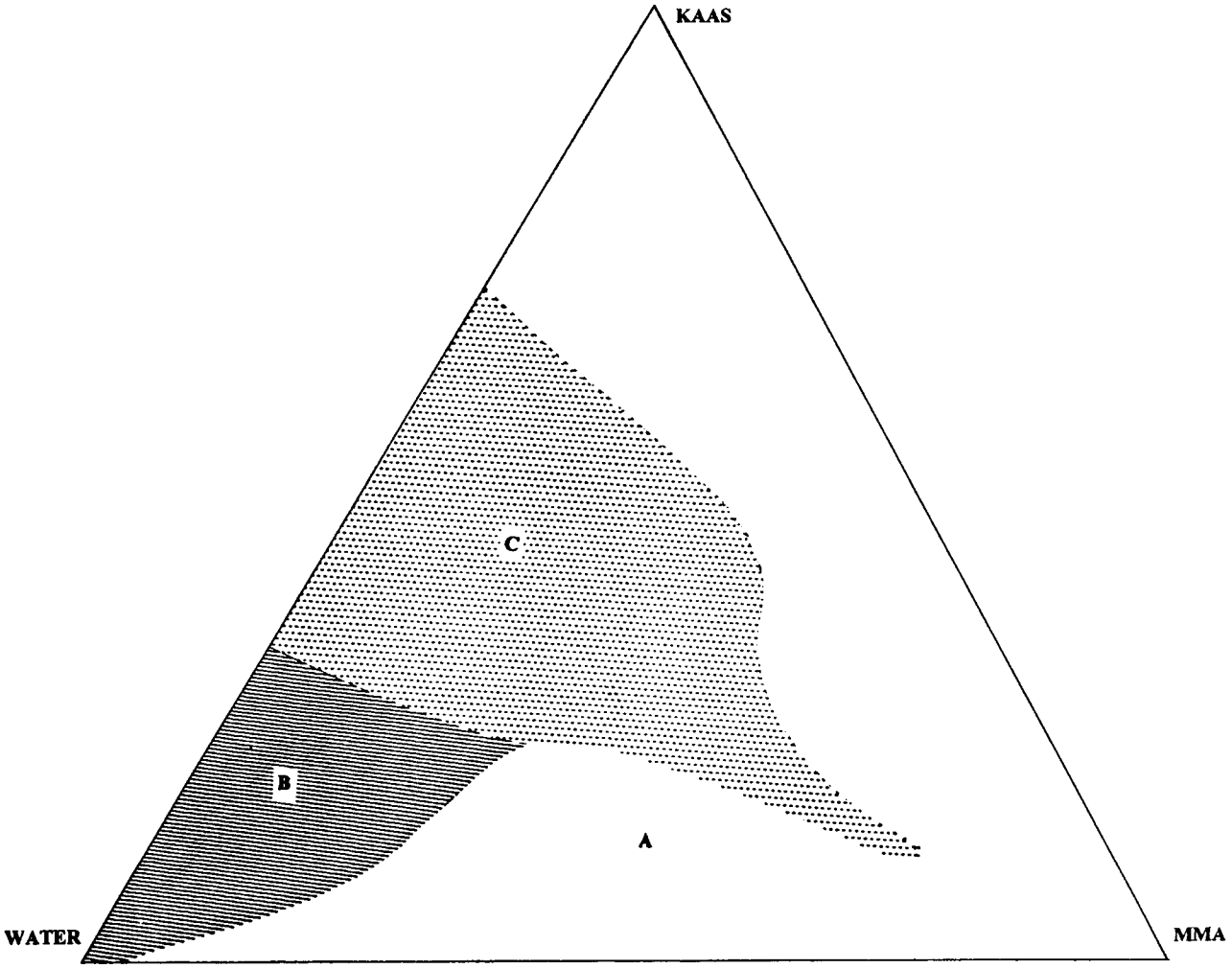

Figure 3 Phase-behavior diagram for the system MMA, EGDMA, KAAS, and water at 25°C. Compositions are on a weight percent basis and the EGDMA content is 5% by weight of MMA. Domains: (A) compositions that were not single phase; (B) thermodynamically stable, transparent single-phase systems; (C) kinetically stable single-phase systems.

radiation and also by thermal techniques.[21] Hence, the use of AIBN enabled the free-radical polymerization of the aqueous foam to be activated by UV radiation and the subsequent completion of polymerization using thermal activation.

Morphology Observation

The morphology of the polymeric foams was examined using a scanning electron microscope (SEM). The samples for SEM observation were prepared by drying the polymeric foam at 55°C followed by microtoming. The foam samples were coated using a Polaron E5400 coating machine and an ISI SX 40 scanning electron microscope was used to study the morphology.

Density Determination

The volume of the dried polymeric foam sample was determined by measuring the sample dimensions. The density of the polymeric foam was then obtained after determining the weight of the sample.

Extraction of Unreacted Monomer and Surfactant

The polymeric foam was dried to constant weight at 55°C to remove moisture. The unconverted reactants were then extracted with water using a Soxhlet extractor for a period of 24 h. The polymeric foam was then dried to constant weight at 55°C. The weight loss on extraction was considered as equal to the weight of unpolymerized reactants. The ex-

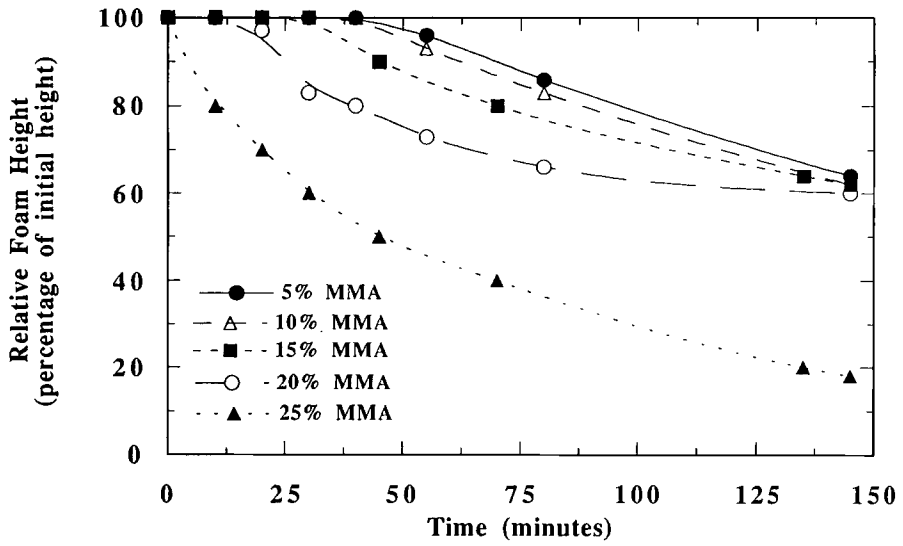

Figure 4 Results of foam stability as a function of MMA content. The results shown were obtained using a constant water : KAAS ratio of 3 : 1, with increasing MMA content. (The MMA used contained 5% by weight of EGDMA.)

traction duration of 24 h was arrived at based on preliminary studies that showed the weight of samples being extracted to remain constant after 16 h of Soxhlet extraction; this was taken to be indicative of the completion of extraction. Further, the high solubility in water of the KAAS homopolymer was observed from its complete dissolution in water at 25°C within 15 min. The results from our earlier studies[24] on photopolymerization of MMA and EGDMA had indicated complete polymerization of the monomers. These observations indicate that this extraction protocol could be satisfactorily used to determine the extractable content of the polymer foams synthesized in this study.

RESULTS

Synthesis and Characterization of KAAS

The yield of acrylamidostearic acid was 70% based on oleic acid. The FTIR spectra for the surfactant KAAS is shown in Figure 2. The IR absorption band at 3100 cm^{-1} indicates the presence of the terminal vinyl group ($CH_2{=}CH-$) after synthesis of the surfactant. The absorptions at 1650 and 1560 cm^{-1} are representative of the amide group ($-CONH-$). The results are similar to those reported in the literature.[17,20] The CMC at 25°C for KAAS was 0.0007 mol/L. The FTIR spectra for the polymer obtained from KAAS after homopolymerization is also shown in Figure 2. The FTIR spectra for the polymerized sample do not show the IR absorption at 3100 cm^{-1} that is characteristic of the terminal vinyl group.

Phase-behavior Study

The results of the phase-behavior study for the system composed of MMA, KAAS, and water, containing EGDMA to the extent of 5% of MMA content, is shown in Figure 3. The phase-behavior diagram could be demarcated into three distinct regions: The unshaded portion (region A) of the phase-behavior diagram represents compositions that were not made up of a single phase. Some of these samples separated into two phases on equilibration, whereas a few of the samples exhibited a viscous appearance similar to gels. This region also includes compositions that contained high amounts of KAAS and were nonhomogeneous due to the presence of undissolved KAAS. The samples pertaining to region B were thermodynamically stable, transparent, single-phase systems. The compositions from region C of the diagram were kinetically stable single-phase systems. The samples from region C exhibited slight turbidity on preparation and separated into two-phase systems when allowed to stand for 48 h.

Stability of Aqueous Foams

Representative results of foam stability studies conducted are shown in Figure 4. The results shown in

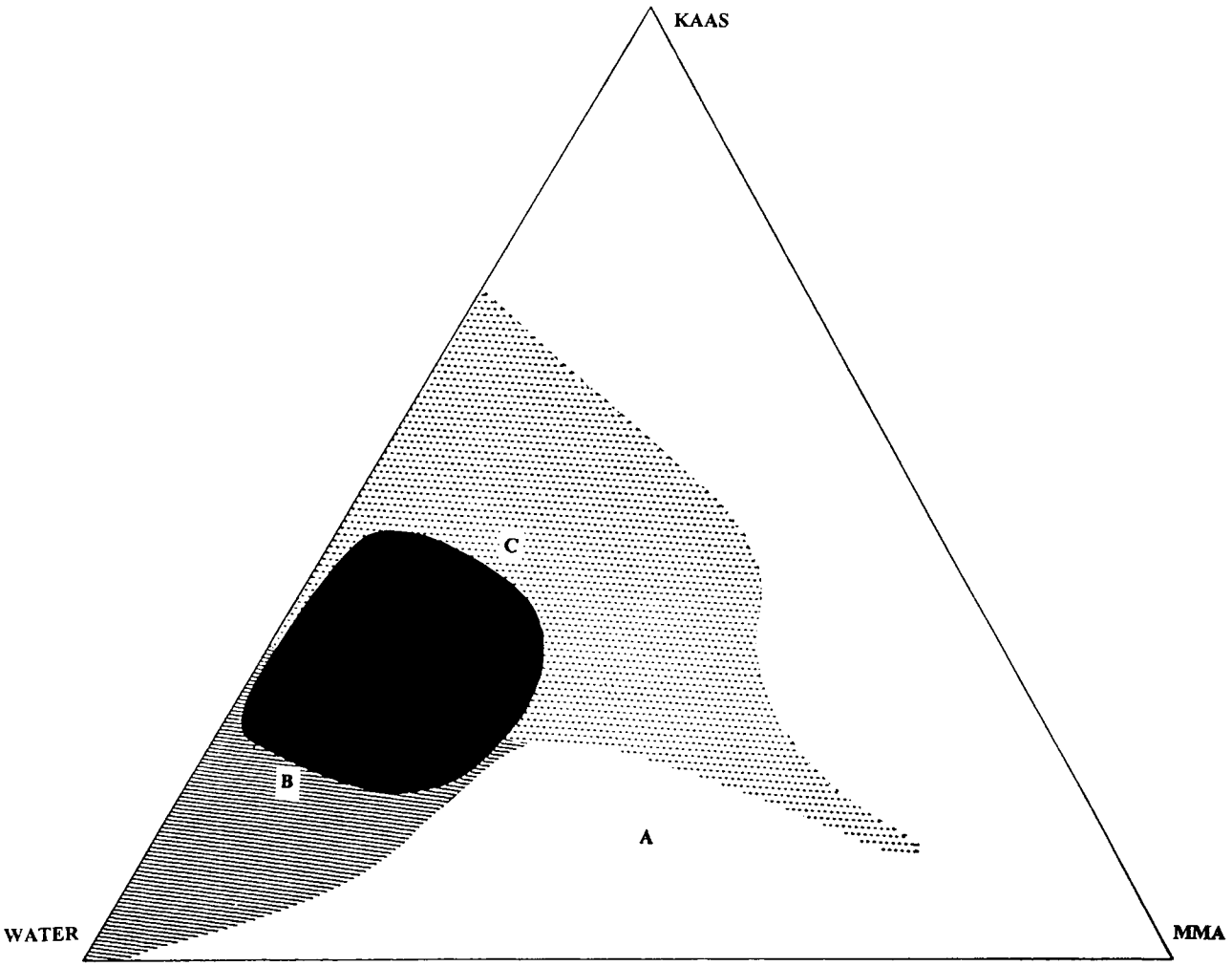

Figure 5 Phase-behavior diagram for the system MMA, EGDMA, KAAS, and water at 25°C showing compositions that yield stable aqueous foams. Compositions are on a weight percent basis and the EGDMA content is 5% by weight of MMA. The darkened region representing compositions that yield stable aqueous foams includes portions of region B (thermodynamically stable, transparent single-phase systems) and region C (kinetically stable single-phase systems). The detailed representation of regions B and C is illustrated in Figure 3. Region A represents compositions that were not single phase.

Figure 4 were obtained using samples containing a constant ratio of water to KAAS of 3 : 1 with varying amounts of MMA. The MMA contained 5% by weight of EGDMA. The foam stability results are represented by plotting the relative foam height (the foam height at any time as a percentage of original height of foam on formation) as a function of time elapsed after foaming for MMA concentrations ranging from 5 to 25%.

Similar foam stability studies were conducted for other compositions pertaining to regions B and C of the phase diagram (Fig. 3) in order to determine compositions that yield stable foams. Compositions that yield stable foams are represented in Figure 5 by the darkened region. Some compositions containing surfactant concentrations greater than 30% could not be foamed using the nitrogen flow conditions used in this study because of high viscosity.

Variation of Viscosity and Surface Tension

The measurement of bulk viscosity and surface tension for representative compositions from the single-phase domain as a function of increasing KAAS

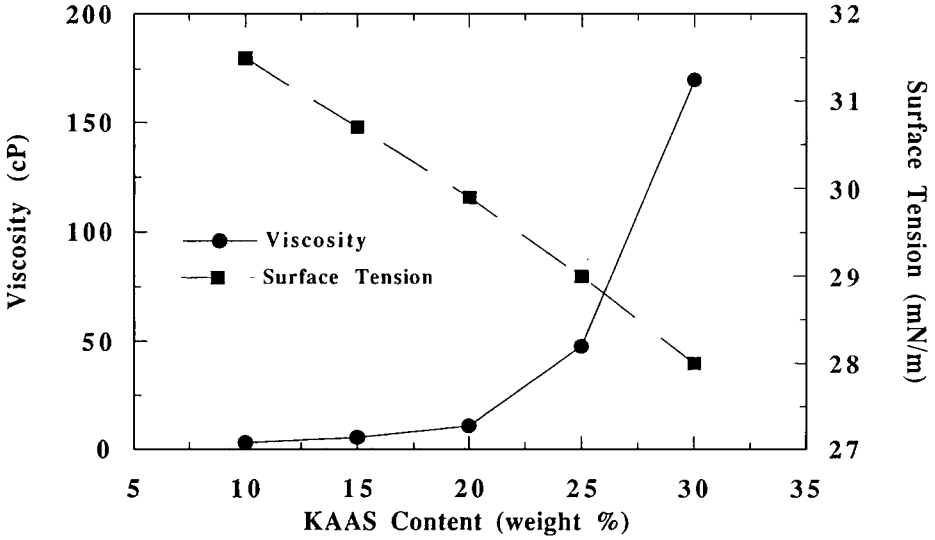

Figure 6 Variation in viscosity and surface tension as a function of increasing KAAS content. The results shown were obtained by maintaining a constant ratio of water to MMA of 9 : 1, with increasing KAAS content.

content of the system is shown in Figure 6. A constant ratio of water to MMA of 9 : 1 was maintained and the KAAS content was varied to obtain the results in Figure 6. The variation in bulk viscosity and surface tension as a function of water content is illustrated in Figure 7 (constant ratio of KAAS : MMA of 9 : 1, increasing water content), whereas Figure 8 shows the variation as a function of MMA content (constant ratio of KAAS : water of 1 : 3, with increasing MMA). The results indicate an increase in bulk viscosity of the aqueous system with increasing KAAS content. The bulk viscosity increases gradually up to 20% KAAS concentration (Fig. 6), followed by a sharp increase at higher KAAS contents. The surface tension decreases almost linearly with increasing KAAS content. On increasing the water content, bulk viscosity decreases sharply up to about 73% water followed by

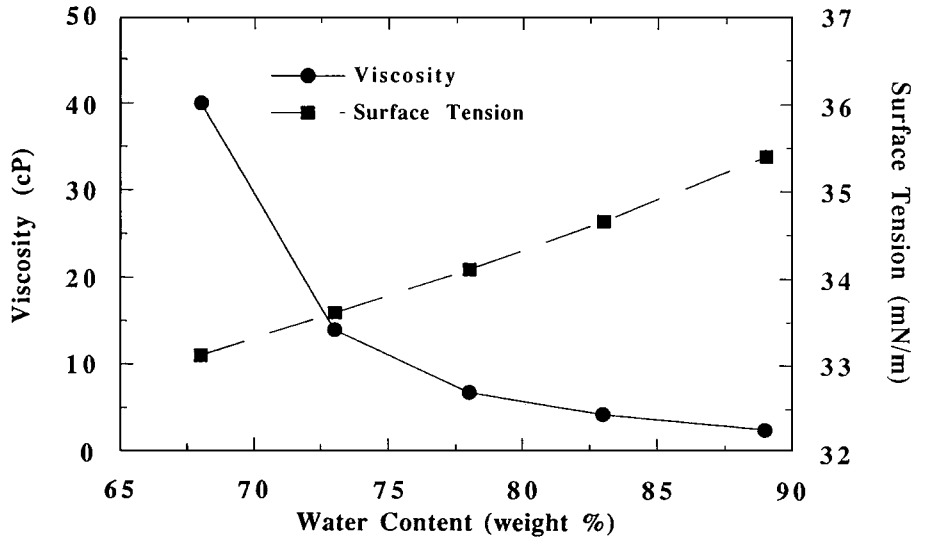

Figure 7 Variation in viscosity and surface tension as a function of increasing water content. The results shown were obtained by maintaining a constant ratio of KAAS to MMA of 9 : 1, with increasing water content.

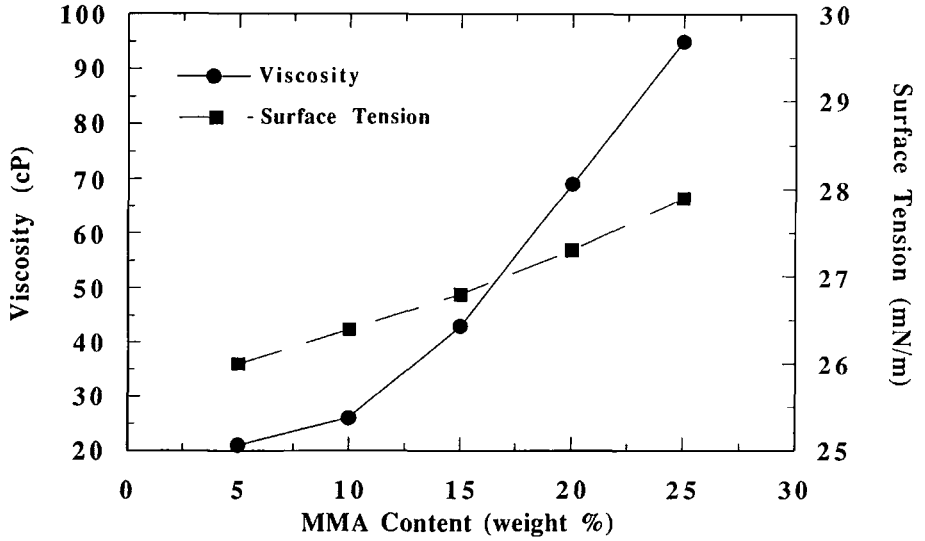

Figure 8 Variation in viscosity and surface tension as a function of increasing MMA content. The results were obtained by maintaining a constant ratio of KAAS to water of 1 : 3, with increasing MMA content.

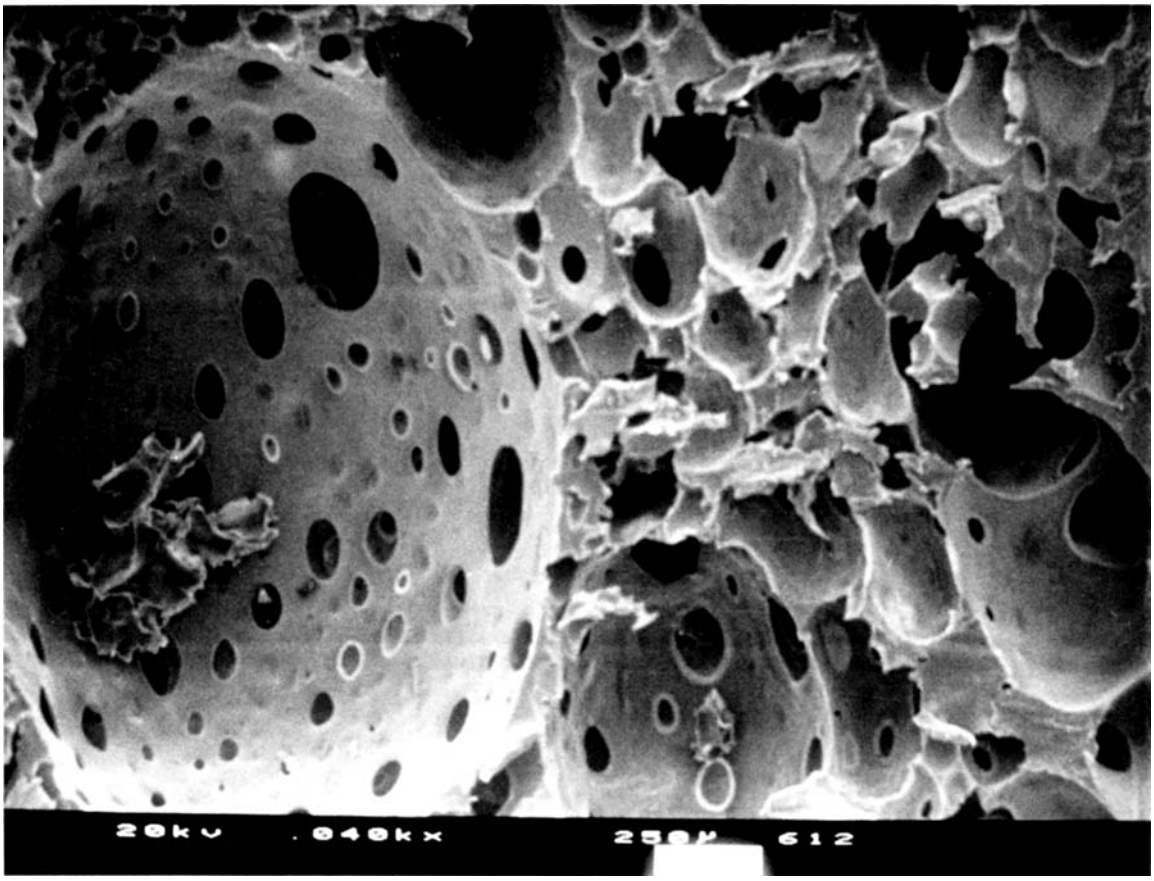

Figure 9 Morphology of polymer foam obtained by polymerizing an aqueous foam formed from a system composed of MMA: 15%, KAAS: 20%, and water: 65% without sonication of the aqueous system during purging with nitrogen. (All compositions are on a weight percent basis and MMA contains 5% by weight of EGDMA.)

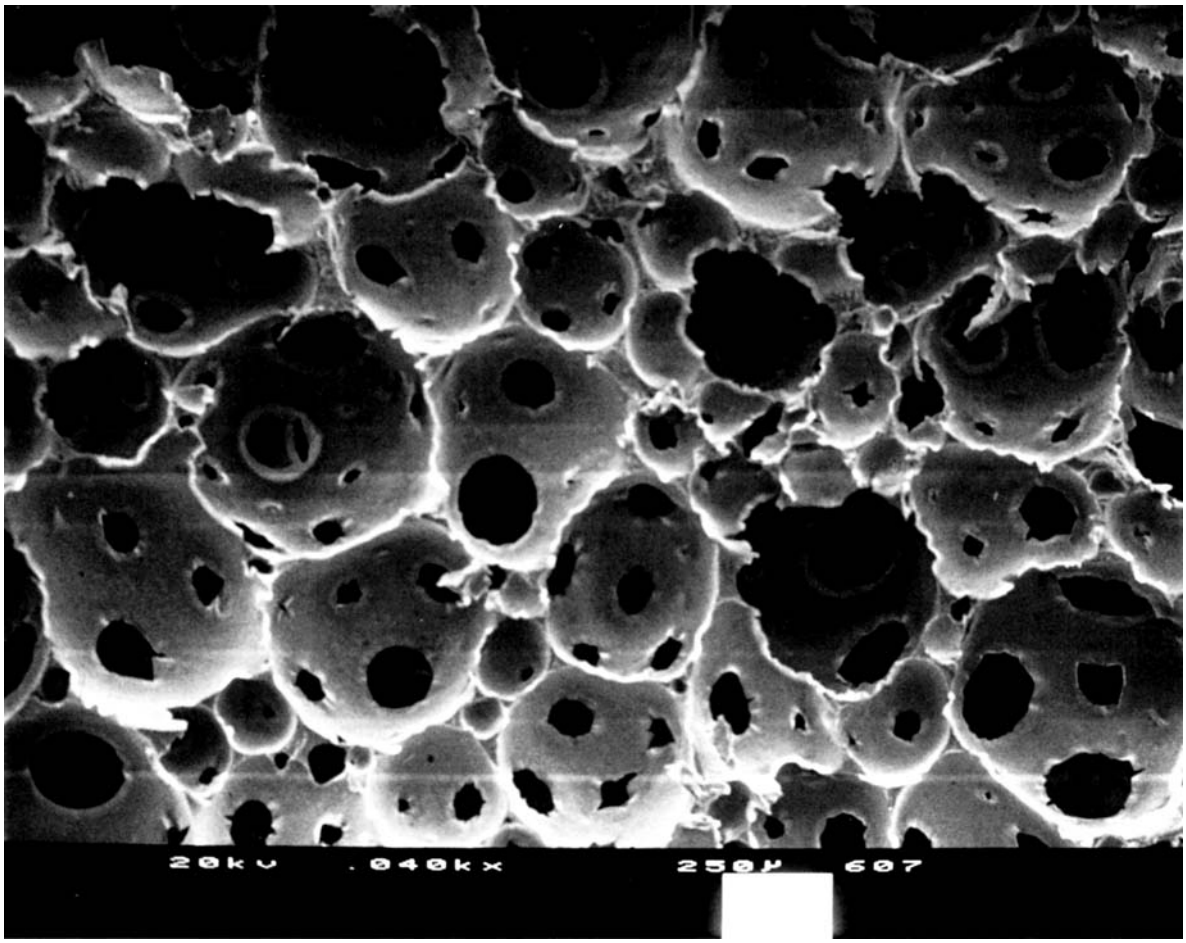

Figure 10 Morphology of polymer foam obtained by polymerizing an aqueous foam formed from a system composed of MMA: 15%, KAAS: 20%, and water: 65% with sonication of the aqueous system during purging with nitrogen. (All compositions are on a weight percent basis and MMA contains 5% by weight of EGDMA.)

a more gradual decrease (Fig. 7). The surface tension increases with increasing water content in an almost linear manner. As the MMA content of the system is increased, both surface tension and bulk viscosity increase (Fig. 8). The surface tension increases gradually in an almost linear manner, whereas the increase in bulk viscosity is sharp at MMA content greater than 10%.

Effect of Sonication

The influence of sonication during formation of the aqueous foam on the morphology of the polymeric foam obtained is illustrated in Figures 9 and 10. The SEM micrograph in Figure 9 represents polymeric foam obtained by purging without sonication a precursor system containing 65% water, 15% MMA, and 20% KAAS, followed by polymerization of the aqueous foam. The polymeric foam obtained exhibits an open-cell porous structure but with wide dispersity in the sizes of the cells (1500–150 μm) as also the number of openings between cells. The SEM micrograph in Figure 10 shows the morphology of polymeric foam from a precursor of the same composition (65% water, 15% MMA, 20% KAAS) but with sonication of the precursor system during foaming with nitrogen. The polymeric foam in Figure 10 also shows an open-cell porous structure but with a more uniform cell size (600–250 μm) and cell structure compared to the polymeric foam in Figure 9. Qualitatively similar results of the effect of sonication on foam morphology were obtained when using precursor systems of other compositions as well.

Table I Details of the Various Polymer Foam Samples Studied: Sample Number, Precursor Composition, Corresponding Figure Illustrating the Foam Morphology, Density of the Polymeric Foam(g/mL), and the Cell-size Range (μm) of the Foam

	Increasing Surfactant →		
	Sample No.		
	1	4	7
Composition	23.75, 71.25, 5	28.5, 66.5, 5	33.25, 61.75, 5
Figure no.	11	14	17
Density	0.12	0.18	0.28
Cell-size range	1500–1100	800–550	600–400
	Sample No.		
	2	5	8
Composition	22.5, 67.5, 10	27, 63, 10	31.5, 58.5, 10
Figure no.	15	15	18
Density	0.21	0.31	0.34
Cell-size range	750–500	650–450	500–350
	Sample No.		
	3	6	9
Composition	20, 60, 20	24, 56, 20	28, 52, 20
Figure no.	13	16	19
Density	0.27	0.36	0.48
Cell-size range	650–450	600–400	350–250
	← Increasing Water		

Increasing MMA ↓

The compositions are listed as percentage by weight in the following order: KAAS, water, MMA. The MMA content listed contains 5% by weight of EGDMA. The trend in composition variation represented by the samples is also indicated in the table.

Morphology of Polymeric Foam

The relationship between the composition of the aqueous precursor and the morphology of the polymeric foam was investigated. The objective of the study was to evaluate the effect of the components of the precursor system (oil, water, and surfactant) on the polymeric foam structure. The compositions used in the study were selected from the region of the phase-behavior diagram that yielded stable aqueous foams (Fig. 5). Some of the compositions, representative of those used in the study along with the figure numbers of the corresponding SEM micrographs, are shown in Table I. Samples 1–3 in Table I represent compositions that were obtained by adding increasing amounts of MMA to a solution containing 75% water and 25% KAAS. Similarly, samples 4–6 were obtained by adding MMA to a 30% solution of KAAS in water and samples 7–9 were obtained by adding MMA to a 35% solution of KAAS in water. The trend in composition variation represented by these samples is also indicated in Table I. The MMA concentration of the samples increases on going from top to bottom in Table I. Water concentration in the samples increases on going from right to left and the surfactant concen-

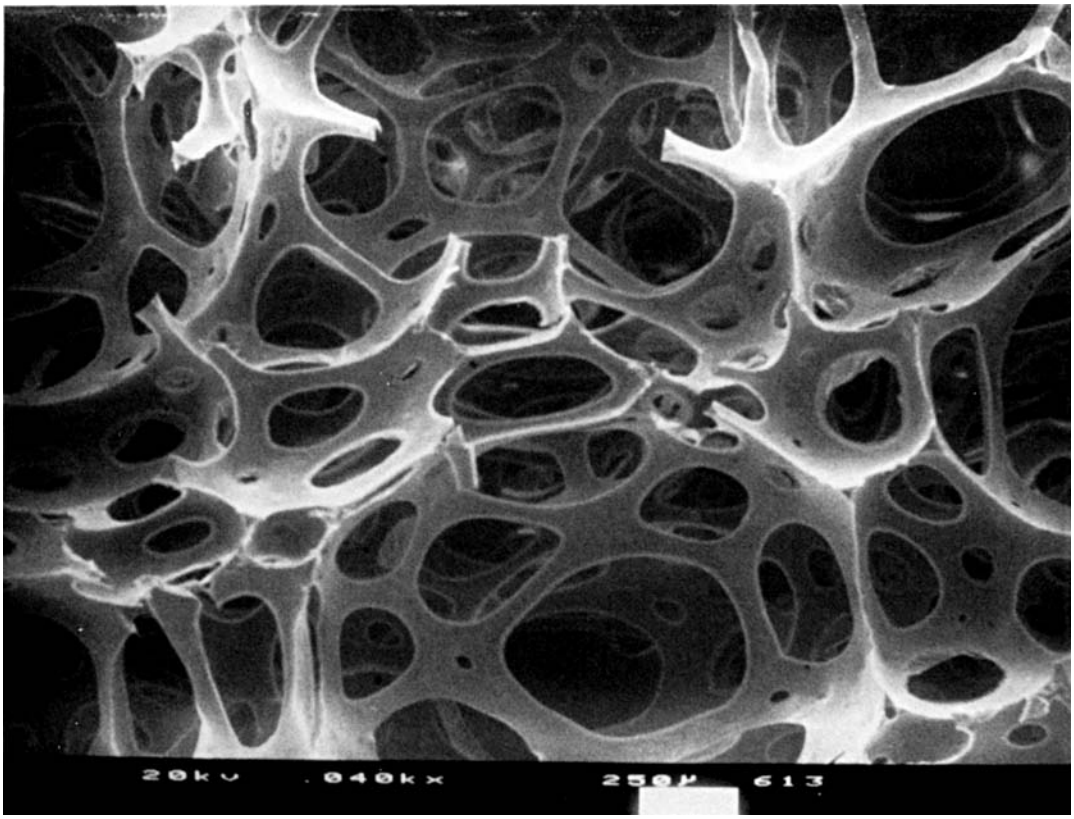

Figure 11 Morphology of polymer foam corresponding to sample 1 of Table I.

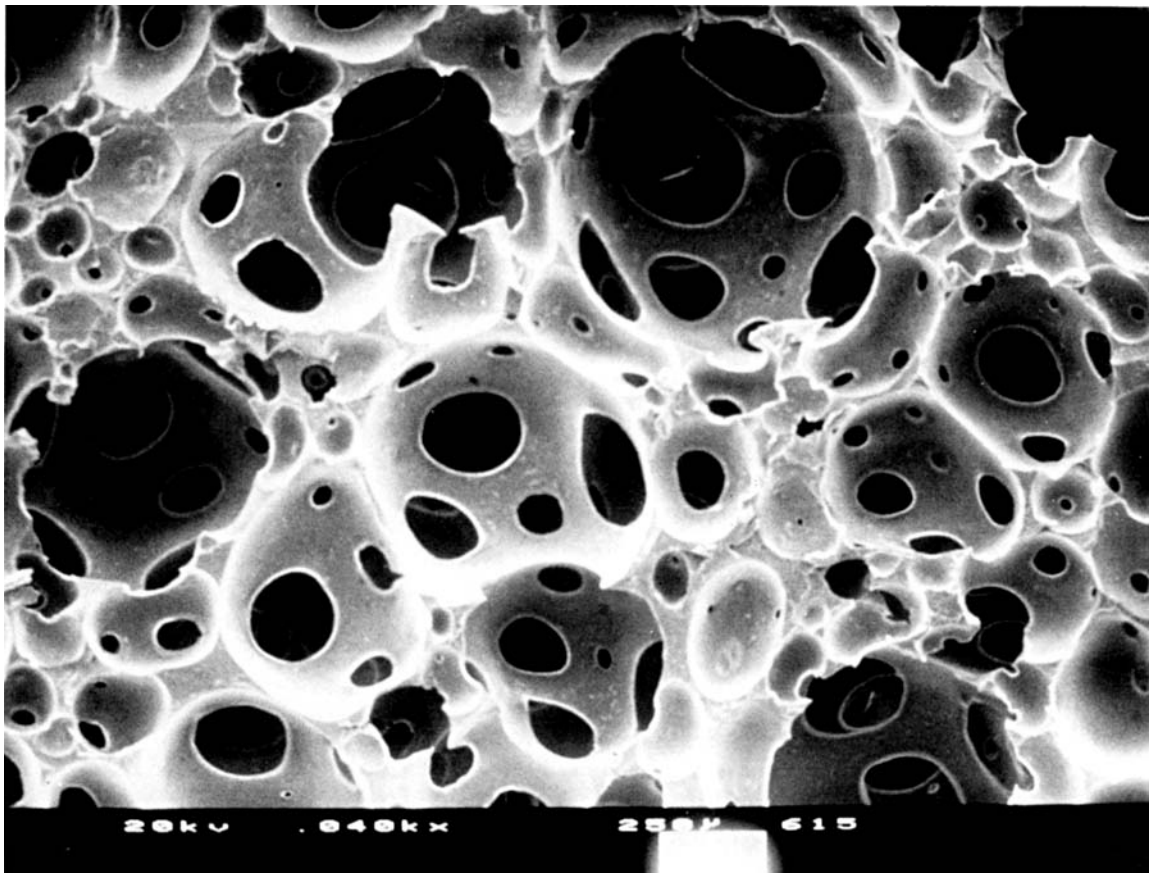

Figure 12 Morphology of polymer foam corresponding to sample 2 of Table I.

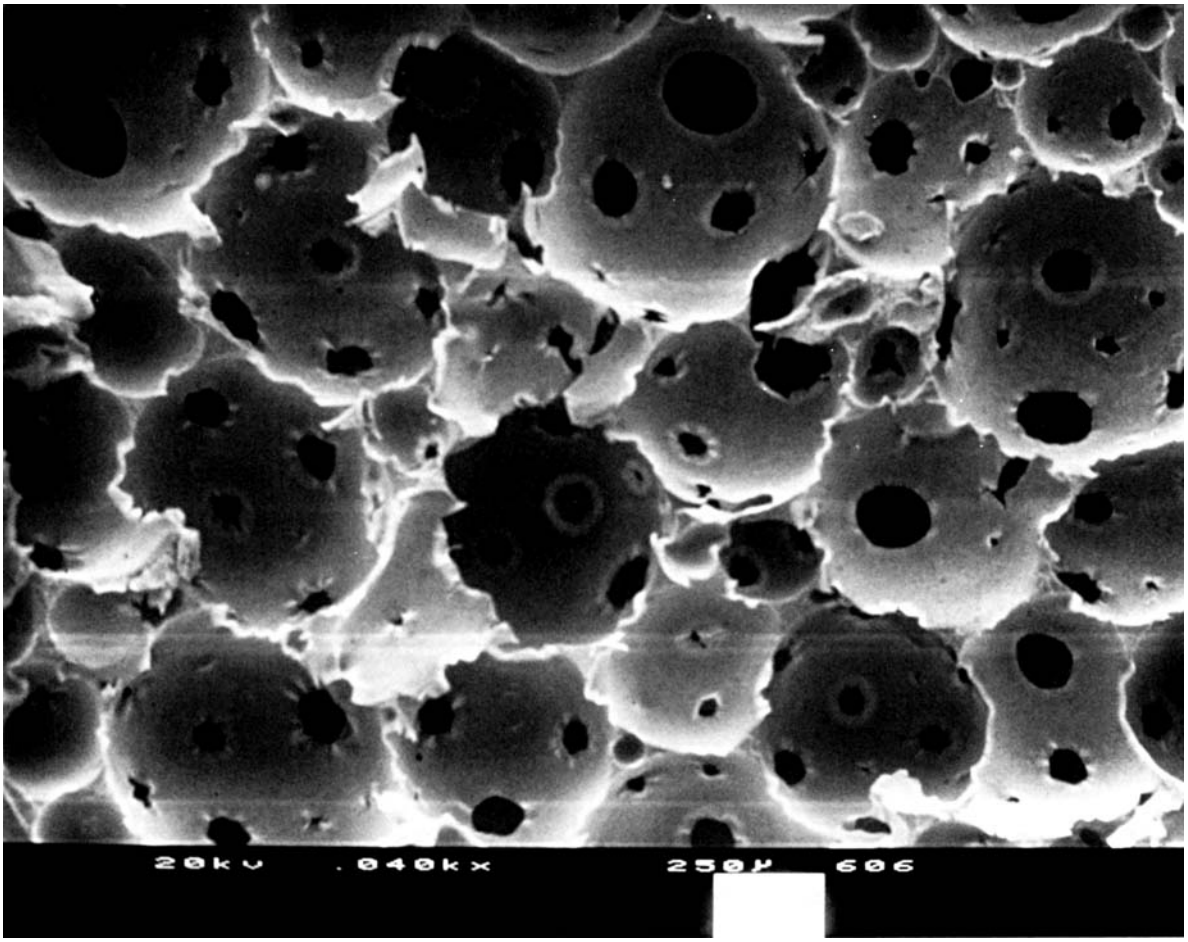

Figure 13 Morphology of polymer foam corresponding to sample 3 of Table I.

tration increases on going from left to right in Table I. A qualitative measure of the influence of the components of the precursor on the morphology of the polymeric foam can thus be evaluated using samples 1–9. The cell size range for samples 1–9 observed from the corresponding SEM micrographs is also included in Table I.

An examination of polymer foam morphology (Figs. 11–19) in conjunction with the composition table (Table I) indicates the following dependence of foam morphology on precursor composition: An increase in surfactant content of the aqueous precursor results in a decrease in cell size of the polymeric foam and also a decrease in the sizes of openings between cells. This is inferred by going from left to right in the composition table (Table I) and observing the corresponding polymer foam morphology (Figs. 11–19). Similarly, it can be inferred that an increase in water content (right to left in Table I) results in an increase in the size of the cells and also the size of openings between cells. With increasing MMA content of the precursor (top to bottom in Table I), the cell size and also the sizes of openings between cells appear to decrease.

Density of Polymeric Foam

The densities of the polymeric foams corresponding to samples 1–9 are also listed in Table I. The results of foam densities from Table I in conjunction with the composition data for the corresponding precursor system indicates an increase in polymeric foam density with increasing MMA content. The foam density is also found to increase with increasing surfactant content. In contrast, the density of polymeric foam obtained decreases with increasing water content of the precursor.

Extractable Content of Polymeric Foam

The amount of unconverted reactants determined by Soxhlet extraction with water was found to be

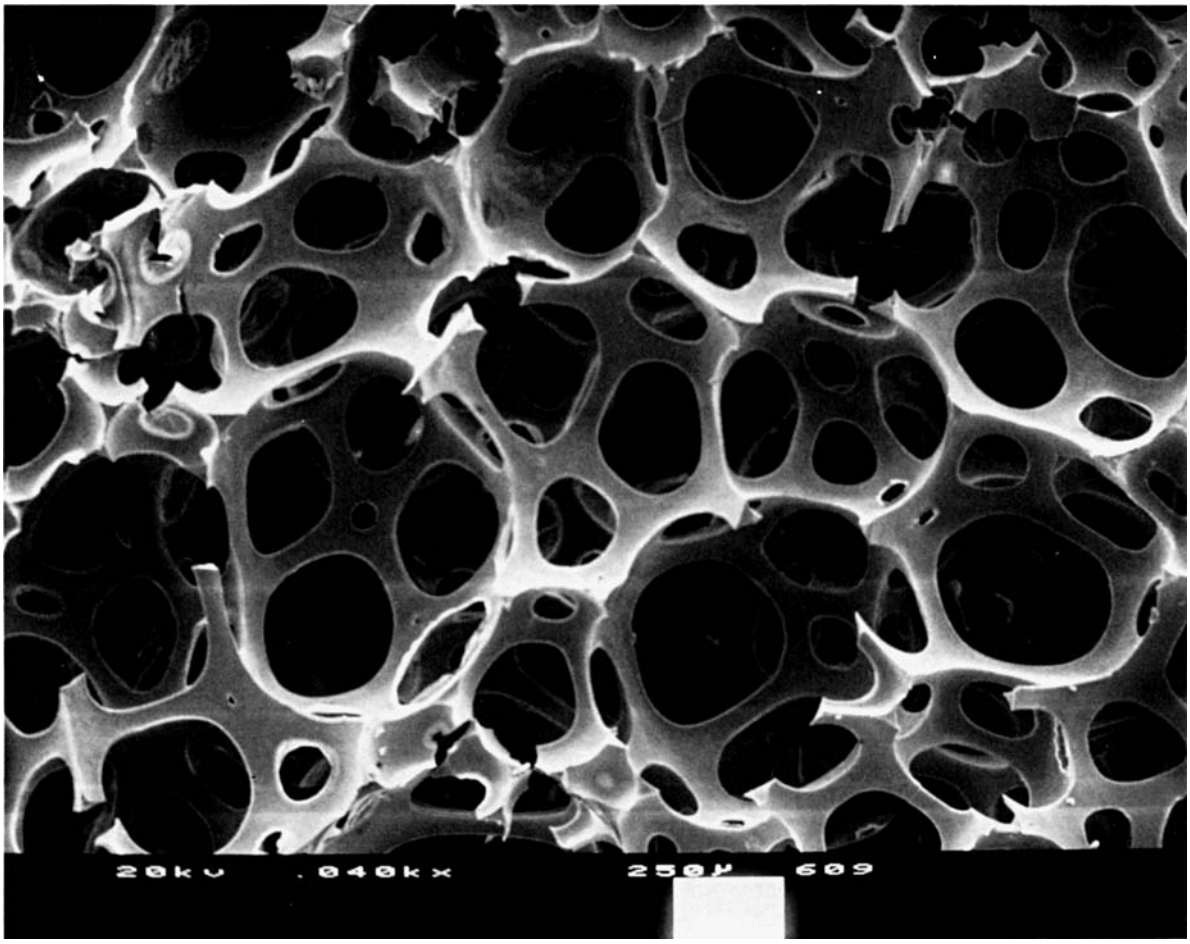

Figure 14 Morphology of polymer foam corresponding to sample 4 of Table I.

less than 0.5% by weight for all foams obtained from the region of stable foam composition. This indicates the almost complete polymerization of the monomer, cross-linking agent, and surfactant present in the precursor system.

DISCUSSION

The polymerization of oleic acid does not yield polymer of very high molecular weight due to an autoinhibition effect[22] resulting from the presence of allylic hydrogen in the molecule. The allylic hydrogen causes highly active chain transfer reactions during free-radical polymerization, thereby forming low molecular weight polymer. The observation of this behavior in the polymerization of oleic acid and also undecylenic acid has been reported.[17,20,23] Hence, the chemical modification of oleic acid to acrylamidostearic acid was carried out. AAS obtained using the modified Ritter reaction is a saturated fatty acid with a side group of acrylamide attached to the stearate chain. The acrylamide side group is attached to the stearate chain at the carbon atom that had allylic hydrogen present in oleic acid. The IR spectra of KAAS shows the presence of a terminal vinyl group and also the existence of the amide group. This indicates the presence of the acrylamide group. These results are in agreement with the results reported in literature on the characterization of AAS based on proton NMR and IR spectroscopic studies.[17,20] In AAS, the terminal vinyl group present in the acrylamide side group is not subject to allylic inhibition and this enables the formation of high molecular weight polymer. The neutralization of AAS with KOH helps to introduce the potassium head group that imparts amphiphilic character to the molecule. Consequently, KAAS behaves as a polymerizable surfactant. The absence of IR absorption corresponding to the terminal vinyl group in the case of the homopolymerized surfactant (Fig. 2) is in-

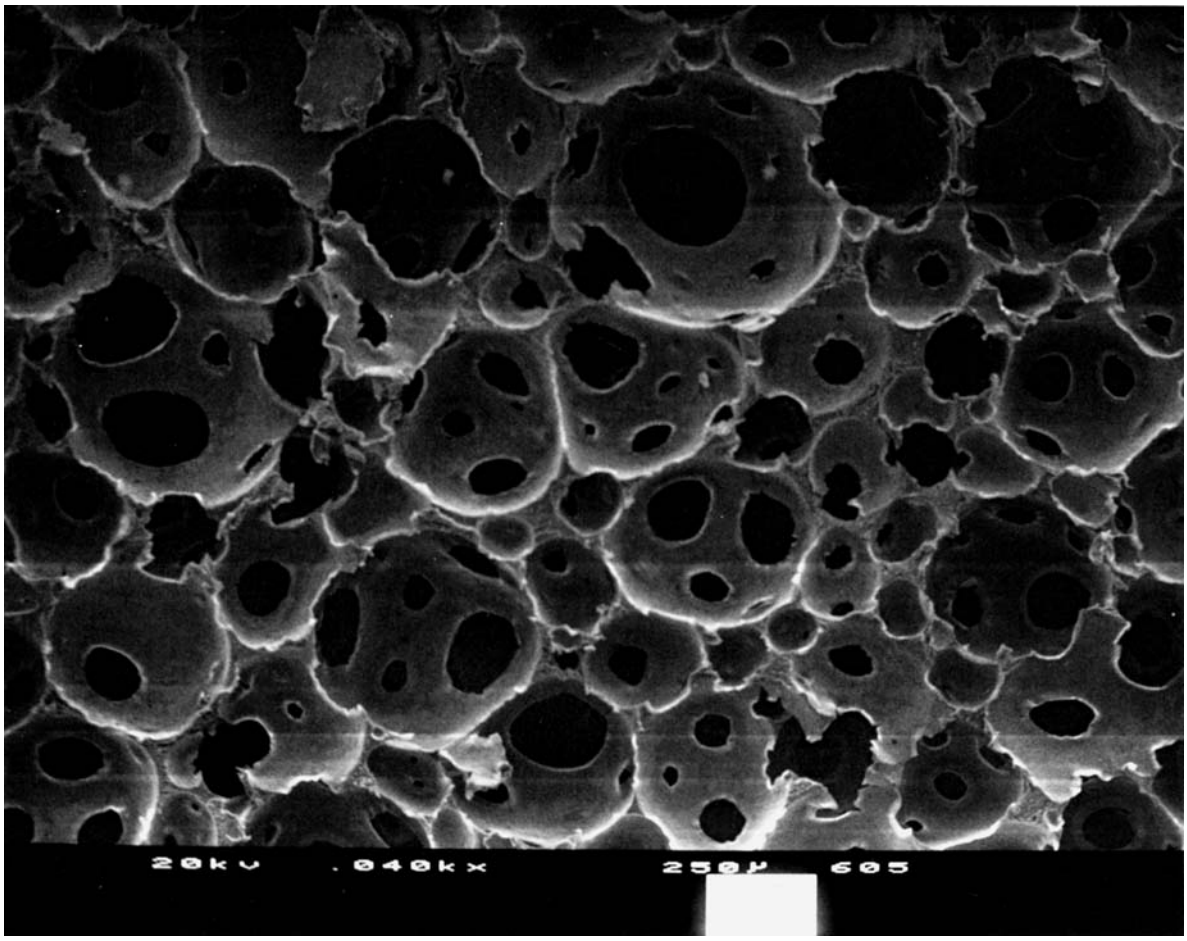

Figure 15 Morphology of polymer foam corresponding to sample 5 of Table I.

dicative of the polymerization reaction undergone by the surfactant.

The compositions yielding a stable foam represents a portion of regions B and C in the phase diagram (Fig. 5). The stability of the foam formed would be dependent on the rate of drainage of liquid from the foam. The foams obtained from compositions pertaining to the darkened portion of the phase diagram (Fig. 5) appear to exhibit drainage kinetics favorable for the stability of foams. An explanation of this can be obtained from the results of viscosity and surface tension measurements (Figs. 6–8). With increasing surfactant concentration, the bulk viscosity increases and surface tension decreases (Fig. 6). The decrease in surface tension could result in an increase in surface viscosity.[18] The combination of increasing bulk and surface viscosity could result in reduced draining of the foams.[18,19] This suggests that foam stability would increase with increasing surfactant concentration, as has been observed experimentally in this study. However, a limiting factor is the sharp increase in bulk viscosity at surfactant concentrations above 25% that hinders the formation of foams by the foaming technique employed in this study. Hence, there exists a boundary in the phase diagram for the stable foam region at high surfactant concentrations (Fig. 5). On increasing the water content, the bulk viscosity decreases and surface tension increases (Fig. 7). The increase in surface tension with water content could lower the surface viscosity. This effect combined with a reduction in bulk viscosity could increase drainage of liquid from the foam, thereby destabilizing the foam. This is experimentally observed with the region of stable foam not extending above 80% water concentration (Fig. 5). Increasing the MMA content of the system causes an increase in bulk viscosity and an increase in surface tension. The increase in bulk viscosity would be favorable to foam stability, but an increase in surface tension with a corresponding decrease in surface viscosity would be unfavorable. Hence, foam stability begins to decrease at MMA

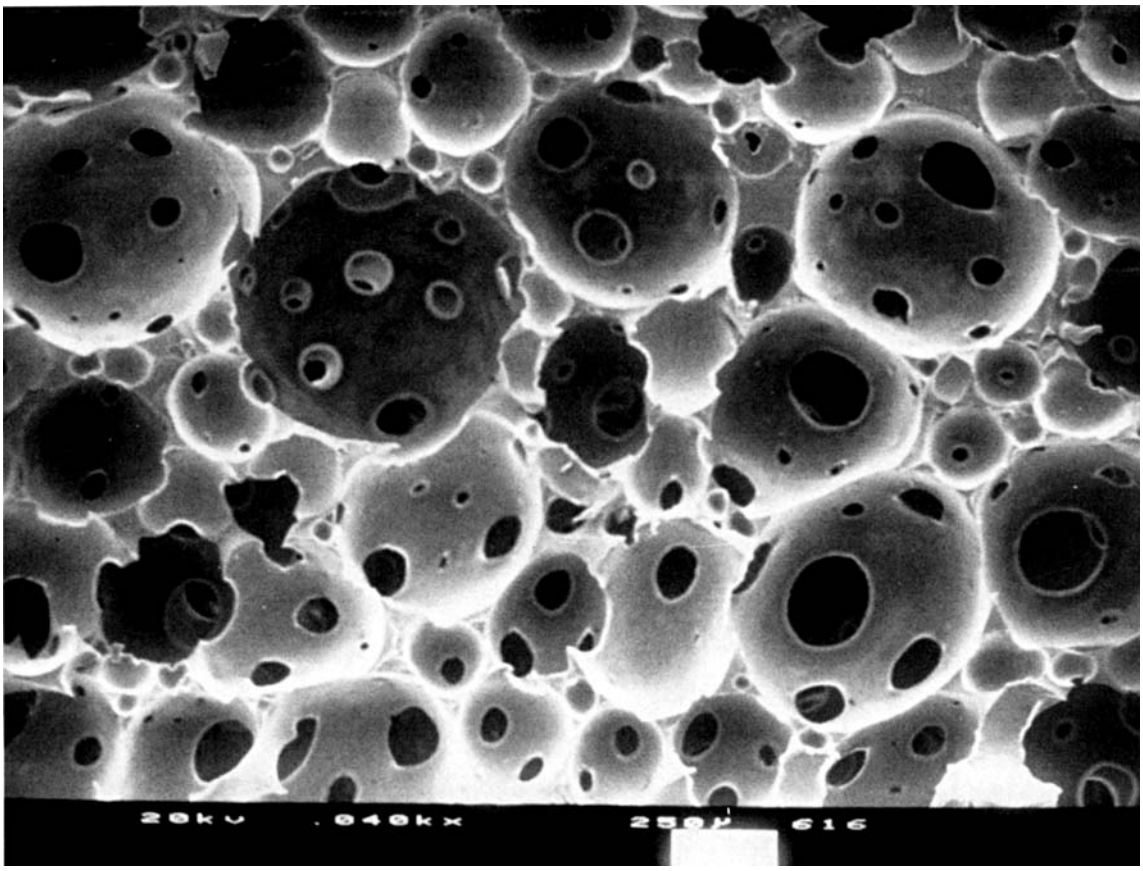

Figure 16 Morphology of polymer foam corresponding to sample 6 of Table I.

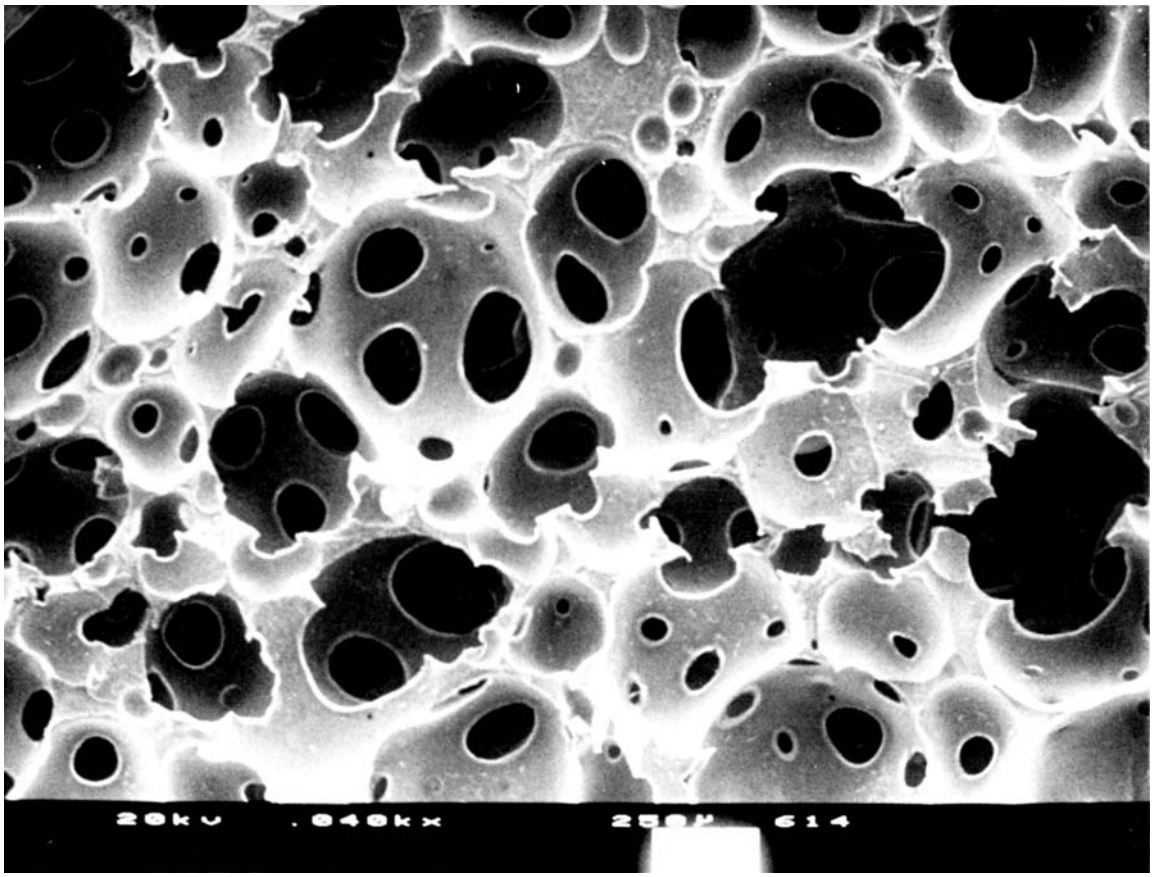

Figure 17 Morphology of polymer foam corresponding to sample 7 of Table I.

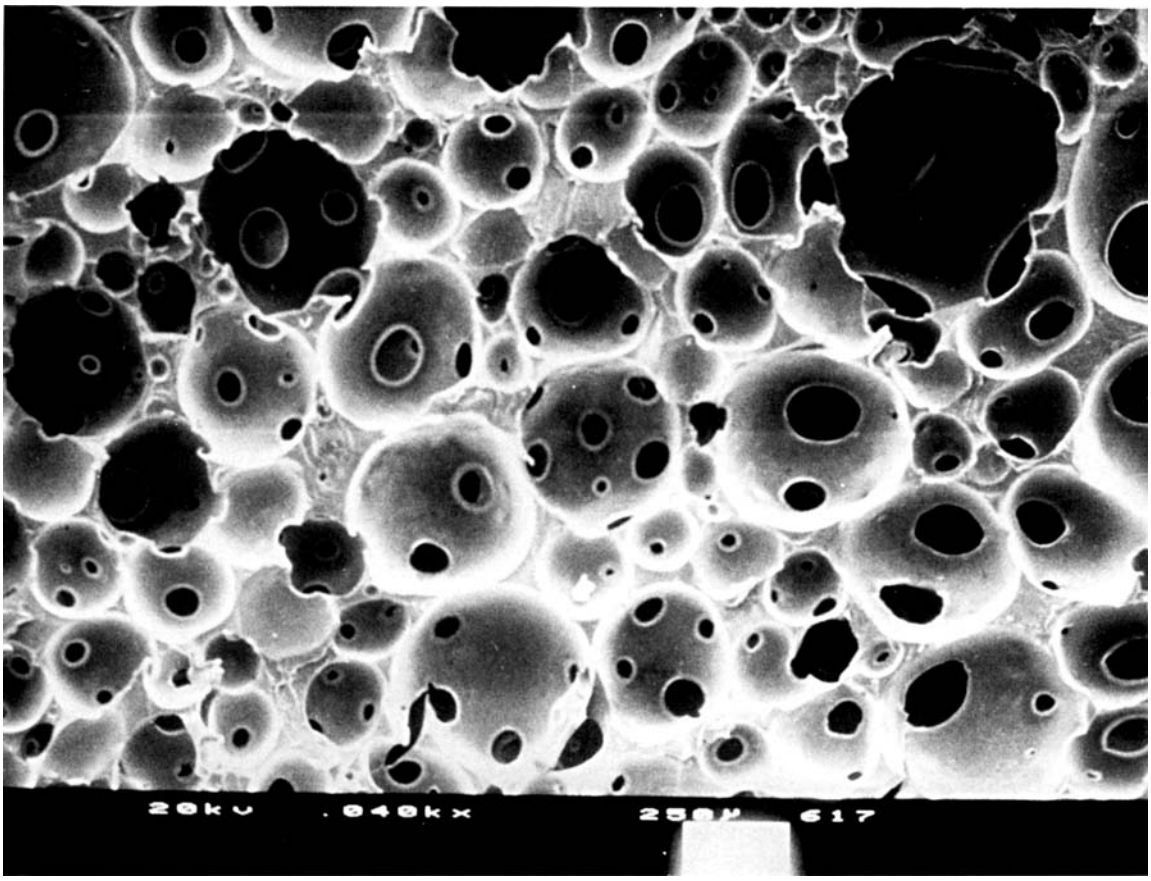

Figure 18 Morphology of polymer foam corresponding to sample 8 of Table I.

content above 25% as observed from the region of stable foams (Fig. 5). This behavior is also evident from the results of the foam stability study (Fig. 4), which show a sharp decrease in the stability of foams at MMA concentrations around 25%.

A comparison of the morphology of the polymeric foams illustrated in Figures 9 and 10 clearly indicates the positive effect of sonicating the system during foaming on the uniformity of cell structure and size in the polymeric foam. Sonicating the aqueous precursor during purging with nitrogen would cause some of the less stable foam cells formed to collapse. New cells would then be generated from the drained liquid by the foaming action of nitrogen being purged. This dynamic process of the formation and collapse of foam cells results in a narrowing of the size distribution of cells constituting the foam and a more uniform foam structure. The actual size of the aqueous foam cells would be dependent on the characteristics of the precursor, the conditions of nitrogen purging, and sonication. The process of cell collapse could also occur during polymerization of the aqueous foam, thereby broadening the size distribution of the foam cells. Hence, the morphology of the polymeric foam would be dependent on both the structure of the aqueous foam and also structural changes occurring during polymerization. Based on the experimental results obtained, the foam formed with sonication exhibits a more uniform morphology compared to foam formed without sonication.

The dependence of foam morphology on precursor composition can be explained based on the results of viscosity and surface tension variations with composition. With increasing surfactant concentration, the bulk viscosity increases and the surface tension decreases. This could result in a reduced rate of drainage and a more stable aqueous foam. The increased stability of the foam would reduce the rate of cell collapse, yielding a foam with a smaller cell size since collapse of cells usually causes an upward shift in the cell size distribution.[18] This, in turn, could lead to smaller cells in the polymeric foam obtained on polymerization of the aqueous foam. Further, the surfactant used is also polymerizable and so functions as a comonomer with MMA. An increase in surfactant concentration is equivalent

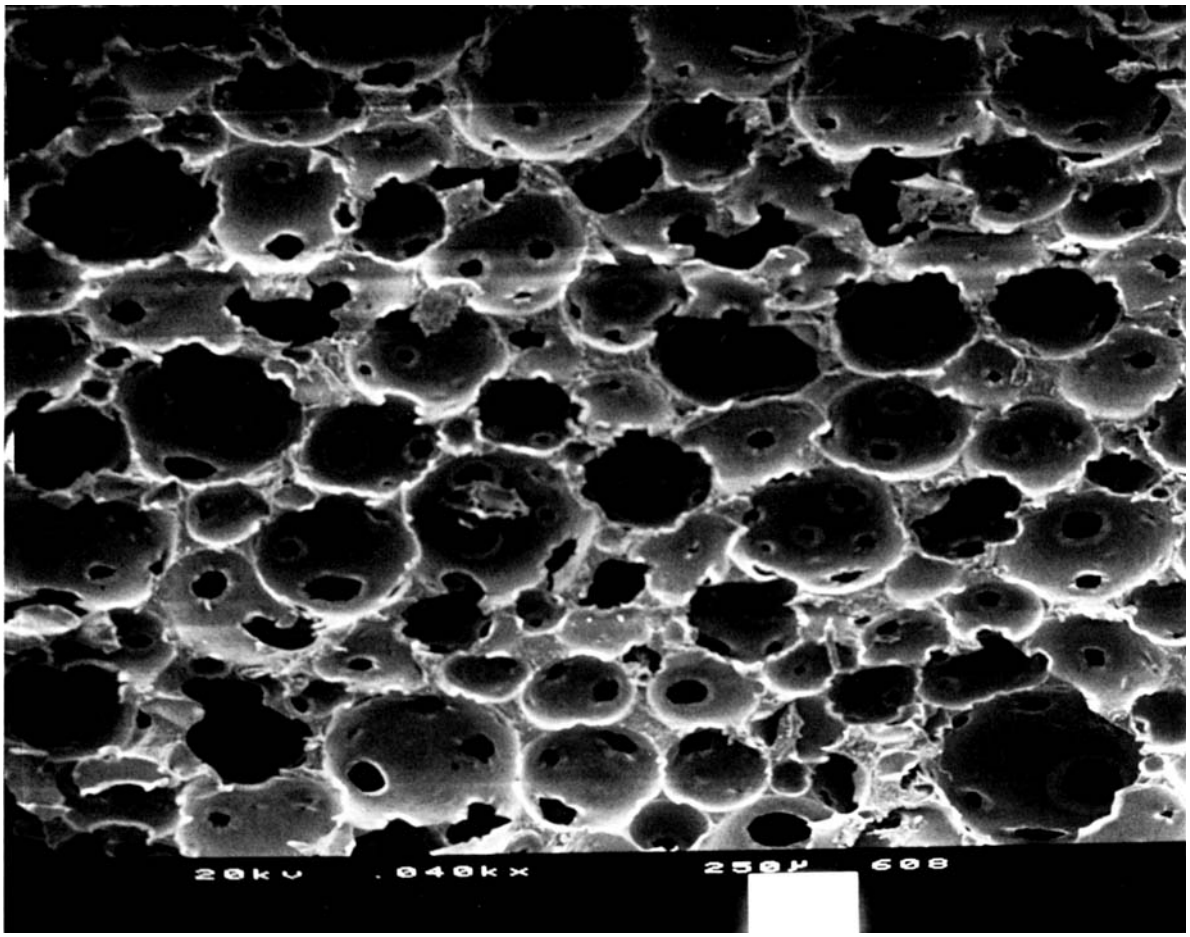

Figure 19 Morphology of polymer foam corresponding to sample 9 of Table I.

to increasing the monomer content of the precursor. This could contribute to the smaller size of the openings between cells with increasing surfactant concentration as the polymerizable fraction of the precursor is higher.

Similarly, the effect of water content of the aqueous precursor on the morphology of the polymeric foam can be explained based on bulk viscosity and surface tension of the systems. The bulk viscosity decreases with increasing water content and the surface tension increases. This could lead to a less stable aqueous foam due to an increase in the rate of drainage and larger cell sizes resulting from a higher rate of cell collapse. Water present in the aqueous precursor represents a nonpolymerizable component and so an increase in water content results in larger sizes of openings between cells. These factors explain the morphology of the polymeric foam obtained from precursors containing high water contents. This is supported by observation of the foam morphology; for example, in Figure 11, at high water, low surfactant, and low MMA content, the structure of the polymeric foam is observed to be composed of only struts, with cell walls virtually absent.

On increasing the MMA content of the precursor up to 20%, the viscosity increases sharply and surface tension decreases marginally (Fig. 8). The morphology of the polymeric foam indicates a decrease in both the cell size and the sizes of openings between cells with increasing MMA content up to 20%. The results of the morphology study in conjunction with the results of viscosity and surface tension measurements indicates the sharp increase in viscosity up to MMA content of 20% to be primarily responsible for the smaller cell size. This could be due to greater stability of the aqueous foam with increasing viscosity. The marginal decrease in surface tension does not appear to adversely affect foam stability. The observed decrease in the sizes

of openings between cells with increasing MMA content up to 20% can be attributed to the increase in the polymerizable content of the precursor system.

The results of polymeric foam densities (Table I) can be explained based on the morphology of the foams. On increasing the water content of the precursor, the foam obtained has a more open structure. The increase in voids results in a smaller amount of polymer per unit volume, resulting in a reduction in foam density. With increasing MMA content or surfactant content, the morphology of the polymeric foam is made of smaller cells having smaller openings. Hence, the amount of polymer in a unit volume of foam increases, yielding higher foam densities.

CONCLUSION

The cell size in the polymeric foams obtained was found to vary significantly depending on the composition of the precursor. The cell size was found to be inversely related to the surfactant content of the precursor. The sizes of the openings between the cells increased with increasing water content of the precursor but decreased with increasing monomer content. The density of the foams varied from 0.12 to 0.48 g/mL and was found to be inversely dependent on the cell size and the size of openings between the cells. The incorporation of the polymerizable surfactant in the polymeric foam was confirmed by the low amount of hot-water extractables (less than 0.5%) in the foam. This technique represents a route that could have technological significance in the formation of polymeric foams with control of the density and pore structure.

REFERENCES

1. K. W. Suh and D. D. Webb, in *Encyclopedia of Polymer Science and Engineering,* 2nd ed., H. F. Mark, N. M. Bikales, C. G. Overberger, and G. Menges, Eds., Wiley, New York, 1987, Vol. 3, p. 1.
2. J. D. C. Wilson, U.S. Pat. 2,772,995 (1956) (to E. I. du Pont de Nemour).
3. J. H. Aubert, *J. Cell. Plast.,* **24,** 132 (1988).
4. J. H. Aubert and R. L. Clough, *Polymer,* **26,** 2048 (1988).
5. C. L. Jackson and M. T. Shaw, *Polymer,* **31,** 1070 (1990).
6. R. W. Pekala and R. E. Stone, *Polym. Prepr.,* **29**(1), 204 (1988).
7. D. K. Swatling, J. A. Manson, D. A. Thomas, and L. H. Sperling, *J. Appl. Polym. Sci.,* **26,** 591 (1981).
8. G. Srinivasan and J. R. Elliott, *Ind. Eng. Chem. Res.,* **31**(5), 1414 (1992).
9. J. M. Williams, *Langmuir,* **7,** 1370 (1991).
10. S. E. Friberg and J. Fang, *J. Colloid Interface Sci.,* **118**(2), 543 (1987).
11. J. M. Williams, A. J. Gray, and M. H. Wilkerson, *Langmuir,* **6,** 437 (1990).
12. M. L. Litt, B. R. Hsieh, I. M. Krieger, T. T. Chen, and H. K. Lu, *J. Colloid Interface Sci.,* **115**(2), 312 (1987).
13. J. M. Williams and D. A. Wrobelski, *Langmuir,* **4,** 656 (1988).
14. D. Barby and Z. Haq, Eur. Pat. 0,060,138 (1982) (to Unilever).
15. J. M. Williams, *Langmuir,* **4,** 44 (1988).
16. B. W. Greene, D. P. Sheetz, and T. D. Filer, *J. Colloid. Interface Sci.,* **32**(1), 90 (1970).
17. L. M. Gan and C. H. Chew, *J. Dispersion Sci. Tech.,* **5**(2), 179 (1984).
18. J. H. Clint, in *Surfactant Aggregation,* Chapman and Hall, New York, 1992, p. 253.
19. P. C. Hiemenz, in *Principles of Colloid and Surface Chemistry,* Marcel Dekker, New York, 1986, p. 385.
20. C. H. Chew and L. M. Gan, *J. Polym. Sci. Polym. Chem. Ed.,* **23,** 2225 (1985).
21. F. Candau, Z. Zekhnini, and J. Durand, *J. Colloid Interface Sci.,* **114**(2), 398 (1986).
22. G. Odian, in *Principles of Polymerization,* 2nd ed.; Wiley, New York, 1981, p. 250.
23. W. R. Palani Raj, M. Sasthav, and H. M. Cheung, *Langmuir,* to appear.
24. W. R. Palani Raj, M. Sasthav, and H. M. Cheung, *Langmuir,* **7,** 2586 (1991).
25. W. R. Palani Raj, M. Sasthav, and H. M. Cheung, *J. Appl. Polym. Sci.,* to appear.
26. M. Sasthav and H. M. Cheung, *Langmuir,* **7,** 1378 (1991).

Received September 17, 1992
Accepted December 21, 1992